T. Setälä, J. Lindberg, K. Blomstedt, J. Tervo, and A. T. Friberg, Coherent-mode representation of a statistically homogeneous and isotropic electromagnetic field in spherical volume, Physical Review E 71, 036618 (2005).

http://link.aps.org/abstract/pre/v71/p036618

Coherent-mode representation of a statistically homogeneous and isotropic electromagnetic field in spherical volume

Tero Setälä,* Jari Lindberg, and Kasimir Blomstedt
Department of Engineering Physics and Mathematics, Helsinki University of Technology, P.O. Box 3500, FI-02015 HUT, Finland

Jani Tervo
LightTrans GmbH, Wildenbruchstrasse 15, D-07745 Jena, Germany

Ari T. Friberg
Department of Microelectronics and Information Technology, Royal Institute of Technology, SE-164 40 Kista, Sweden
(Received 14 December 2004; published 22 March 2005)

It is known that statistically stationary, homogeneous, and isotropic source distributions generate, in an unbounded low-loss medium, an electromagnetic field whose electric cross-spectral density tensor is proportional to the imaginary part of the infinite-space Green tensor. Using the recently established electromagnetic theory of coherent modes, we construct, in a finite spherical volume, the coherent-mode representation of the random electromagnetic field having this property. The analysis covers the fundamental case of blackbody radiation but is valid more generally; since a thermal equilibrium condition is not invoked, the electromagnetic field may have any spectral distribution. Within the scalar theory of coherent modes, which has been available for more than two decades, the analogous formulation results in the first explicit three-dimensional coherent-mode representation.

DOI: 10.1103/PhysRevE.71.036618 PACS number(s): 03.50.De, 42.25.−p

I. INTRODUCTION

In the investigations of partial optical coherence in random scalar wave fields in the space-frequency domain, the theory of coherent modes plays a central role both from the practical and the fundamental point of view [1,2]. Although the theory is more than 20 years old, apart from a few exceptions [3,4], it has mainly been applied to two-dimensional (or beamlike) scalar fields. Furthermore, a rigorous formulation of the coherent-mode theory for general electromagnetic fields has not been available, until very recently [5,6].

In this work, we apply the theory of coherent modes, both in the scalar and electromagnetic formulation, to certain specific three-dimensional, statistically stationary, homogeneous, and isotropic fields. More explicitly, we construct, in a finite spherical volume, the coherent-mode representation for the scalar and vectorial light fields whose cross-spectral density at any frequency is proportional to the imaginary part of the infinite-space Green function or tensor. This form of the cross-spectral density is obtained for the fields generated by statistically homogeneous and isotropic source distributions within a low-loss medium; scalar and electromagnetic treatments are found in Refs. [7–9] and Ref. [10], respectively. For example, the electric cross-spectral density tensor of blackbody radiation belongs to this class of cross-spectral tensors [11–13]. But in our analysis no thermal equilibrium needs to be assumed, and the field therefore may have an arbitrary spectrum. From a physical point of view, the fields that we consider correspond to a superposition of isotropically distributed and angularly uncorrelated random plane waves [14], which in the electromagnetic case further are completely unpolarized [15].

In the scalar case, the derivation of the coherent-mode representation relies on making use of a known expansion of the diverging spherical wave. On the other hand, the electromagnetic analysis is based on expanding the infinite-space Green tensor in terms of both transverse and longitudinal spherical vector wave functions by means of the Ohm-Rayleigh method. In both cases, the distribution and shapes of the modes are demonstrated.

The paper is arranged as follows. Section II is a concise overview of the scalar theory of coherent modes. In Sec. III the theory is applied to random scalar fields whose cross-spectral density function is proportional to the imaginary part of the infinite-space Green function. Section IV introduces briefly the electromagnetic theory of coherent modes, which then in Sec. V is employed for vector fields having the electric cross-spectral density tensor proportional to the infinite-space Green tensor. For readability, the mathematical details have been collected, in a self-contained manner, into Appendixes A–D.

II. COHERENT-MODE REPRESENTATION OF SCALAR FIELDS

We begin with a brief summary of the basic concepts pertaining to the coherent-mode representation of fluctuating, statistically stationary scalar fields. At any frequency ω, the coherence properties of the field at two points in space, $\mathbf{r}_1$ and $\mathbf{r}_2$, are described by the cross-spectral density function, defined by the Fourier transform

*Email address: Tero.Setala@hut.fi; FAX: +358 9 451 3155.

$$W(\mathbf{r}_1,\mathbf{r}_2,\omega) = \frac{1}{2\pi}\int_{-\infty}^{\infty} \Gamma(\mathbf{r}_1,\mathbf{r}_2,\tau)\exp(i\omega\tau)\mathrm{d}\tau, \tag{1}$$

where

$$\Gamma(\mathbf{r}_1,\mathbf{r}_2,\tau) = \langle U^*(\mathbf{r}_1,t)U(\mathbf{r}_2,t+\tau)\rangle \tag{2}$$

is the mutual coherence function. The function $U(\mathbf{r},t)$ is the complex analytic signal associated with the random scalar field, and the asterisk and angle brackets denote complex conjugation and averaging, respectively. The function $\Gamma(\mathbf{r}_1,\mathbf{r}_2,\tau)$ characterizes the field correlations between the two points at time difference τ.

The scalar cross-spectral density functions are Hermitian and non-negative definite Hilbert-Schmidt kernels, and therefore they admit the following Mercer series representation (Ref. [1], Sec. 4.7.1):

$$W(\mathbf{r}_1,\mathbf{r}_2,\omega) = \sum_n \alpha_n(\omega)\psi_n^*(\mathbf{r}_1,\omega)\psi_n(\mathbf{r}_2,\omega). \tag{3}$$

The quantities $\alpha_n(\omega)$ and $\psi_n(\mathbf{r},\omega)$ are the eigenvalues and eigenfunctions, respectively, of a homogeneous Fredholm integral equation of the second kind,

$$\int_D W(\mathbf{r}_1,\mathbf{r}_2,\omega)\psi_n(\mathbf{r}_1,\omega)\mathrm{d}^3r_1 = \alpha_n(\omega)\psi_n(\mathbf{r}_2,\omega), \tag{4}$$

where the integration is performed over the domain D (not necessarily finite) under consideration. If we define the inner product of two functions $a(\mathbf{r})$ and $b(\mathbf{r})$ over D to be

$$\{a(\mathbf{r}),b(\mathbf{r})\}_D \equiv \int_D a^*(\mathbf{r})b(\mathbf{r})\mathrm{d}^3r, \tag{5}$$

the set of eigenfunctions can be chosen to be orthonormal, i.e.,

$$\{\psi_m(\mathbf{r},\omega),\psi_n(\mathbf{r},\omega)\}_D = \delta_{mn}, \tag{6}$$

where δ_{mn} is the Kronecker delta. The factors $\psi_n(\mathbf{r},\omega)$ satisfy the Helmholtz equation, and thus each term in the summation in Eq. (3) likewise obeys a pair of Helmholtz equations. Since the terms in the summation are of a spatially factored form, they represent elementary modes which are completely coherent, and therefore Eq. (3) is called the coherent-mode representation of the cross-spectral density function [1,2].

III. COHERENT-MODE REPRESENTATION OF A HOMOGENEOUS AND ISOTROPIC SCALAR WAVE FIELD

Consider next specifically the statistically homogeneous and isotropic scalar fields, whose cross-spectral density function is proportional to the imaginary part of the infinite-space Green function [7–9,14], i.e., to a sinc function. This functional form is found for the cross-spectral density of the wave field generated by any homogeneous and isotropic source distribution within a medium of negligibly small losses [7–9]. Physically such a field is known to correspond to an isotropic distribution of angularly uncorrelated plane waves [14].

The cross-spectral density function that we consider is explicitly written as

$$W(\mathbf{r}_1,\mathbf{r}_2,k) = \frac{(4\pi)^2 a(k)}{k}\,\mathrm{Im}[G(\mathbf{r}_1,\mathbf{r}_2,k)], \tag{7}$$

where the coefficient $a(k)$ can be interpreted as the spectral density of the plane waves in the plane-wave representation [14]. Further, $k=\sqrt{\epsilon}\omega/c_0$ is the wave number of light, ϵ is the relative permittivity of the linear, homogeneous, and isotropic medium, assumed to have vanishingly small absorption, and c_0 is the speed of light in vacuum. Moreover,

$$G(\mathbf{r}_1,\mathbf{r}_2,k) = \frac{\exp(ik|\mathbf{r}_1-\mathbf{r}_2|)}{4\pi|\mathbf{r}_1-\mathbf{r}_2|} \tag{8}$$

is the infinite-space Green function, whose imaginary part (when k is real) is a sinc function,

$$\mathrm{Im}[G(\mathbf{r}_1,\mathbf{r}_2,k)] = \frac{\sin(k|\mathbf{r}_1-\mathbf{r}_2|)}{4\pi|\mathbf{r}_1-\mathbf{r}_2|}. \tag{9}$$

We note that the function $G(\mathbf{r}_1,\mathbf{r}_2,k)$ is here called the infinite-space Green function, but when $\epsilon=1$ it is usually referred to as the free-space Green function.

In the following, we construct the coherent-mode representation for the cross-spectral density function given in Eq. (7). Although $W(\mathbf{r}_1,\mathbf{r}_2,k)$ in Eq. (7) is for an infinite space, the expression that we derive is interpreted as the coherent-mode representation in a *finite* spherical volume D, of radius d. By making use of Eqs. (A5) and (A8), we can directly write in the spherical polar coordinates

$$W(\mathbf{r}_1,\mathbf{r}_2,k) = (4\pi)^2 a(k)\sum_{n=0}^{\infty}\sum_{m=-n}^{n} j_n(kr_1)j_n(kr_2) \times Y_n^{m*}(\theta_1,\varphi_1)Y_n^m(\theta_2,\varphi_2), \quad \mathbf{r}_1,\mathbf{r}_2 \in D, \tag{10}$$

where $j_n(kr)$ and $Y_n^m(\theta,\varphi)$ are spherical Bessel functions and spherical harmonics, respectively. Next we define the functions

$$\phi_{mn}(\mathbf{r},k) \equiv j_n(kr)Y_n^m(\theta,\varphi), \quad -n \leqslant m \leqslant n, \tag{11}$$

which are known to be solutions of the Helmholtz equation

$$\nabla^2\phi_{mn}(\mathbf{r},k) + k^2\phi_{mn}(\mathbf{r},k) = 0, \tag{12}$$

and are finite at the origin (Ref. [16], Sec. 9.6). With the help of Eq. (A6), the functions $\phi_{mn}(\mathbf{r},k)$ are found to be orthogonal in D, i.e.,

$$\{\phi_{mn}(\mathbf{r},k),\phi_{m'n'}(\mathbf{r},k)\}_D = C_n(k)\delta_{mm'}\delta_{nn'}, \tag{13}$$

where

$$C_n(k) \equiv \int_0^d r^2 j_n^2(kr)\mathrm{d}r = \frac{d^3}{2}[j_n^2(kd) - j_{n-1}(kd)j_{n+1}(kd)]. \tag{14}$$

The first expression in Eq. (14) and Eq. (A10) indicate that if $d\to\infty$, then $C_n(k)\to\infty$, which is one of the reasons for con-

sidering a finite volume. The latter expression in Eq. (14) is obtained from Eq. (A11). For later purposes, we define the functions

$$\psi_{mn}(\mathbf{r},k) \equiv \frac{1}{\sqrt{C_n(k)}} j_n(kr) Y_n^m(\theta,\varphi), \tag{15}$$

which constitute an orthonormal set of functions in D, i.e.,

$$\{\psi_{mn}(\mathbf{r},k), \psi_{m'n'}(\mathbf{r},k)\}_D = \delta_{mm'}\delta_{nn'}. \tag{16}$$

Note that the orthogonality is due solely to the orthogonality with respect to the angular coordinates. Furthermore, the shapes of the functions $\psi_{mn}(\mathbf{r},k)$ are independent of the size of the volume, only the normalization factors $C_n(k)$ depend on it.

In terms of the functions $\psi_{mn}(\mathbf{r},k)$, we can now express the cross-spectral density function of Eq. (10) in the form

$$W(\mathbf{r}_1,\mathbf{r}_2,k) = \sum_{n=0}^{\infty} \sum_{m=-n}^{n} \lambda_n^{(1)}(k) \psi_{mn}^*(\mathbf{r}_1,k) \psi_{mn}(\mathbf{r}_2,k), \tag{17}$$

where

$$\lambda_n^{(1)}(k) = (4\pi)^2 a(k) C_n(k). \tag{18}$$

Using Eq. (16), one readily finds that the functions $\lambda_n^{(1)}(k)$ of Eq. (18) and $\psi_{mn}(\mathbf{r},k)$ of Eq. (15) are, respectively, the eigenvalues and the orthonormal eigenfunctions of the second-kind Fredholm integral equation whose kernel is the cross-spectral density function given in Eq. (17). Consequently, Eq. (17) is, within a spherical domain of radius d, the coherent-mode representation of the cross-spectral density function which is proportional to the imaginary part of the infinite-space Green function. We remark that often only one index labels the modes, resulting in a single summation in the coherent-mode representation. In this case, however, the use of two indices is appropriate and, therefore, the mode representation consists of two summations. Furthermore, we note that the eigenvalue labeled by index n is $(2n+1)$-fold degenerate. The corresponding $2n+1$ eigenfunctions, i.e., those with the same n but different m, are equally weighted in the mode representation, and are orthonormal as evidenced by Eq. (16).

The spectral density of the field at point $\mathbf{r}$ is obtained directly as

$$S(\mathbf{r},k) = W(\mathbf{r},\mathbf{r},k) = \sum_{n=0}^{\infty} \sum_{m=-n}^{n} \lambda_n^{(1)}(k) |\psi_{mn}(\mathbf{r},k)|^2, \tag{19}$$

which, when integrated over the volume D, yields the total energy of the field in D,

$$\int_D S(\mathbf{r},k) \mathrm{d}^3 r = \sum_{n=0}^{\infty} (2n+1) \lambda_n^{(1)}(k). \tag{20}$$

In obtaining this expression, we employed the facts that the eigenfunctions are normalized and that the eigenvalues are $(2n+1)$-fold degenerate. Substituting the first expression of Eq. (14) into Eq. (18) and then using Eq. (A9), the summation in Eq. (20) can be carried out, resulting in

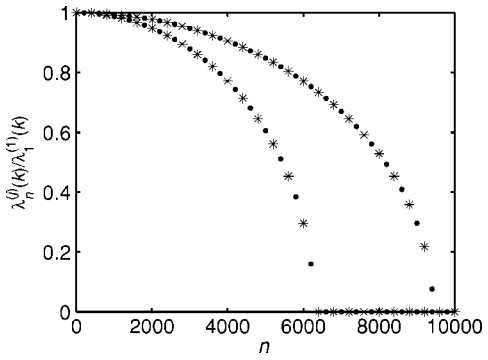

FIG. 1. Behavior of the ratio of eigenvalues $\lambda_n^{(j)}(k)/\lambda_1^{(1)}(k)$ as a function of mode number n for spherical volumes of radius $d=1000\lambda$ (lower curve) and $d=1500\lambda$ (upper curve). Dots are for $j=1$, corresponding to both the scalar and the first set of electromagnetic eigenvalues, whereas stars are for $j=2$, corresponding to the second set of electromagnetic eigenvalues. In both curves, the dots and stars are plotted for modes with number $n=\{200,600,1000,\ldots\}$ and $n=\{1,400,800,\ldots\}$, respectively.

$$\int_D S(\mathbf{r},k) \mathrm{d}^3 r = 4\pi a(k) V_D, \tag{21}$$

where V_D is the volume of the sphere D. Exactly the same result is obtained by setting $\mathbf{r}_1=\mathbf{r}_2$ in Eq. (7) and then integrating the ensuing expression over the volume D.

The distribution of the eigenvalues given by Eq. (18) is illustrated in Fig. 1, where the dots show the behavior of the ratio $\lambda_n^{(1)}(k)/\lambda_1^{(1)}(k)$ as a function of the mode number n. (The stars in Fig. 1 are related to the electromagnetic analysis, and are explained later in Sec. V of the paper.) The lower and upper dot curves correspond to spherical volumes of radius $d/\lambda=1000$ and $d/\lambda=1500$, respectively ($\lambda=2\pi/k$ is the wavelength of the light). Furthermore, for presentational reasons, the ratio $\lambda_n^{(1)}(k)/\lambda_1^{(1)}(k)$ has been computed only for the indices $n=\{200,600,1000,\ldots\}$. It is obvious that the bigger the volume, the more modes are needed to adequately represent the cross-spectral density function. We denote by $n_{\max}$ the maximum value of index n for which the modes contribute significantly to the mode representation, and find from Fig. 1 that $n_{\max}\cong 6300$ for $d/\lambda=1000$, whereas $n_{\max}\cong 9450$ for $d/\lambda=1500$. For other values of radius d/λ, the curves representing the eigenvalues were observed to be similar in shape to those plotted in Fig. 1, and $n_{\max}$ was found to increase linearly with radius d/λ. Since there are $2n+1$ eigenfunctions for each n, the number of significant eigenfunctions is proportional to $(d/\lambda)^2$, i.e., to the surface area of the spherical volume D.

The shapes of the eigenfunctions $\psi_{mn}(\mathbf{r},k)$ are illustrated in Fig. 2, where the squared moduli are shown in polar plots for indices $mn=\{00,01,12\}$. The graphs are for a spherical volume of radius $d/\lambda=1000$, with $kr=10$. In the direction specified by the angles (θ,φ), the value of the function is indicated by the distance from the origin, which is located in the middle of the graph.

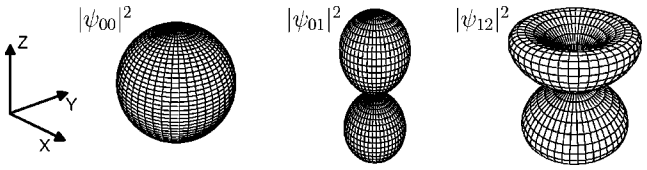

FIG. 2. Illustration of functions $|\psi_{mn}(\mathbf{r},k)|^2$ for indices $mn=\{00,01,12\}$, when the radius of the sphere is $d/\lambda=1000$ and $kr=10$. The value of the function is indicated by the distance from the origin, located in the center of each graph. The orientation of the coordinate axes is shown in the inset.

IV. COHERENT-MODE REPRESENTATION OF ELECTROMAGNETIC FIELDS

The coherent-mode representation of electromagnetic fields is constructed in full analogy to that of the scalar fields. We give here only a brief summary of the theory; for a complete treatment we refer to Ref. [5] (see also Ref. [6]). The coherence properties of a stationary, random electromagnetic field are, at any frequency ω, described by the cross-spectral density tensors [1]. As is customary, we consider in the following only the electric component of the electromagnetic field. The electric cross-spectral density tensor is defined as

$$\overleftrightarrow{W}(\mathbf{r}_1,\mathbf{r}_2,\omega)=\frac{1}{2\pi}\int_{-\infty}^{\infty}\overleftrightarrow{\Gamma}(\mathbf{r}_1,\mathbf{r}_2,\tau)\exp(i\omega\tau)\mathrm{d}\tau, \tag{22}$$

where

$$\overleftrightarrow{\Gamma}(\mathbf{r}_1,\mathbf{r}_2,\tau)=\langle\mathbf{E}^*(\mathbf{r}_1,t)\mathbf{E}(\mathbf{r}_2,t+\tau)\rangle \tag{23}$$

is the electric mutual coherence tensor. The function $\mathbf{E}(\mathbf{r},t)$ is the complex analytic signal representing the electric field vector. As seen from Eq. (23), the tensor $\overleftrightarrow{\Gamma}(\mathbf{r}_1,\mathbf{r}_2,\tau)$ describes the electric-field correlations between two space-time points.

It is readily shown that the electric cross-spectral density tensor satisfies some specific Hermiticity, non-negative definiteness, and square-integrability conditions [5]. These properties imply that it may be expanded as a Mercer series of the form [5,6]

$$\overleftrightarrow{W}(\mathbf{r}_1,\mathbf{r}_2,\omega)=\sum_n\lambda_n(\omega)\boldsymbol{\psi}_n^*(\mathbf{r}_1,\omega)\boldsymbol{\psi}_n(\mathbf{r}_2,\omega),\ \mathbf{r}_1,\mathbf{r}_2\in D, \tag{24}$$

when the inner product for vector-valued complex functions in the volume D (not necessarily finite, in general) is defined to be

$$\{\mathbf{A}(\mathbf{r}),\mathbf{B}(\mathbf{r})\}_D\equiv\int_D\mathbf{A}^*(\mathbf{r})\cdot\mathbf{B}(\mathbf{r})\mathrm{d}^3r. \tag{25}$$

In Eq. (24), the quantities $\lambda_n(\omega)$ and $\boldsymbol{\psi}_n(\mathbf{r},\omega)$ are the eigenvalues and vector-valued eigenfunctions, respectively, of the homogeneous Fredholm integral equation of the second kind,

$$\int_D\boldsymbol{\psi}_n(\mathbf{r}_1,\omega)\cdot\overleftrightarrow{W}(\mathbf{r}_1,\mathbf{r}_2,\omega)\mathrm{d}^3r_1=\lambda_n(\omega)\boldsymbol{\psi}_n(\mathbf{r}_2,\omega). \tag{26}$$

The eigenvalues are real and non-negative, and the eigenfunctions form an orthonormal set in the sense that

$$\{\boldsymbol{\psi}_n(\mathbf{r},\omega),\boldsymbol{\psi}_m(\mathbf{r},\omega)\}_D=\delta_{nm}. \tag{27}$$

Although the orthogonality does not automatically hold if an eigenvalue is degenerate, the corresponding eigenfunctions can always be made orthogonal.

It is straightforward to verify that the factors $\boldsymbol{\psi}_n(\mathbf{r},\omega)$ and the tensors

$$\overleftrightarrow{W}_n(\mathbf{r}_1,\mathbf{r}_2,\omega)=\lambda_n(\omega)\boldsymbol{\psi}_n^*(\mathbf{r}_1,\omega)\boldsymbol{\psi}_n(\mathbf{r}_2,\omega) \tag{28}$$

obey the appropriate Helmholtz equations and Maxwell divergence conditions. In addition, since the tensors $\overleftrightarrow{W}_n(\mathbf{r}_1,\mathbf{r}_2,\omega)$ are of a spatially factored form, they may be understood as elementary cross-spectral density tensors representing completely coherent (and completely polarized [17]) electric fields in the space-frequency domain [18], in the sense of the definition of the spectral degree of coherence for electromagnetic fields [5,18,19],

$$\mu(\mathbf{r}_1,\mathbf{r}_2,\omega)=\frac{\|\overleftrightarrow{W}(\mathbf{r}_1,\mathbf{r}_2,\omega)\|_{\mathrm{F}}}{[\mathrm{tr}\overleftrightarrow{W}(\mathbf{r}_1,\mathbf{r}_1,\omega)]^{1/2}[\mathrm{tr}\overleftrightarrow{W}(\mathbf{r}_2,\mathbf{r}_2,\omega)]^{1/2}}. \tag{29}$$

In this equation

$$\begin{aligned}\|\overleftrightarrow{W}(\mathbf{r}_1,\mathbf{r}_2,\omega)\|_{\mathrm{F}}&=\mathrm{tr}[\overleftrightarrow{W}(\mathbf{r}_1,\mathbf{r}_2,\omega)\cdot\overleftrightarrow{W}^{\dagger}(\mathbf{r}_1,\mathbf{r}_2,\omega)]^{1/2}\\&=\left[\sum_{i,j}|W_{ij}(\mathbf{r}_1,\mathbf{r}_2,\omega)|^2\right]^{1/2},\end{aligned} \tag{30}$$

with the dagger standing for the Hermitian adjoint, denotes the Frobenius norm. Thus, in analogy with the scalar theory, Eq. (24) may be called the coherent-mode representation of the electric cross-spectral density tensor.

V. COHERENT-MODE REPRESENTATION OF A HOMOGENEOUS AND ISOTROPIC ELECTROMAGNETIC WAVE FIELD

Next we consider the specific electromagnetic fields whose electric cross-spectral density tensor is proportional to the imaginary part of the infinite-space Green tensor [10–13,15]. A classic example of such a statistically homogeneous and isotropic random electromagnetic field is the blackbody radiation for which the cross-spectral density tensors already have been known for quite some time [11–13]. Recently, it was demonstrated that all statistically homogeneous and isotropic current source distributions within a low-loss medium, not necessarily those in thermal equilibrium, generate a wave field whose coherence properties are described by the imaginary part of the infinite-space Green tensor [10]. Analogously to the scalar case, such a field may be understood to consist of an isotropic distribution of angularly uncorrelated plane waves which, in addition, are unpolarized [15].

A. Electric cross-spectral density tensor

The electric cross-spectral density tensor that we consider is written as [10–13,15]

$$\overleftrightarrow{W}(\mathbf{r}_1,\mathbf{r}_2,k)=\frac{(4\pi)^2 a(k)}{k}\,\mathrm{Im}[\overleftrightarrow{G}(\mathbf{r}_1,\mathbf{r}_2,k)], \tag{31}$$

with the infinite-space Green tensor given by the expression [20]

$$\overleftrightarrow{G}(\mathbf{r}_1,\mathbf{r}_2,k)=\left(\overleftrightarrow{U}+\frac{1}{k^2}\boldsymbol{\nabla}\,\boldsymbol{\nabla}\right)G(\mathbf{r}_1,\mathbf{r}_2,k). \tag{32}$$

The tensor $\overleftrightarrow{U}$ is the unit tensor and $G(\mathbf{r}_1,\mathbf{r}_2,k)$ is the scalar Green function introduced in Eq. (8). The imaginary part of $\overleftrightarrow{G}(\mathbf{r}_1,\mathbf{r}_2,k)$, for real k, is readily obtained as

$$\mathrm{Im}[\overleftrightarrow{G}(\mathbf{r}_1,\mathbf{r}_2,k)]=\frac{k}{4\pi}\left\{\left[j_0(kR)-\frac{j_1(kR)}{kR}\right]\overleftrightarrow{U}+j_2(kR)\hat{\mathbf{R}}\hat{\mathbf{R}}\right\}, \tag{33}$$

where $\hat{\mathbf{R}}=\mathbf{R}/R$ with $\mathbf{R}=\mathbf{r}_1-\mathbf{r}_2$, and $R=|\mathbf{R}|$. Note that when $4a(k)$ is equal to Planck's law, Eq. (31) is identical with the cross-spectral density tensor of blackbody radiation.

B. Spherical vector wave functions

As in the scalar case, we consider the field in a spherical volume, which suggests us to introduce the spherical vector wave functions [20–24]. They are constructed from the scalar functions $\phi_{mn}(\mathbf{r},k)$ of Eq. (11) as follows:

$$\mathbf{L}_{mn}(\mathbf{r},k)=\frac{1}{k}\boldsymbol{\nabla}\,\phi_{mn}(\mathbf{r},k), \tag{34}$$

$$\mathbf{M}_{mn}(\mathbf{r},k)=\boldsymbol{\nabla}\times[\phi_{mn}(\mathbf{r},k)\mathbf{r}], \tag{35}$$

$$\mathbf{N}_{mn}(\mathbf{r},k)=\frac{1}{k}\boldsymbol{\nabla}\times\boldsymbol{\nabla}\times[\phi_{mn}(\mathbf{r},k)\mathbf{r}]. \tag{36}$$

Note that when $n=0$, so that necessarily also $m=0$, the two latter functions are equal to zero, as can be seen from the explicit forms given in Eqs. (B2) and (B3). However, unless otherwise stated, the equations that we encounter are formally valid for $n=0$ as well. Functions $\mathbf{M}_{mn}(\mathbf{r},k)$ and $\mathbf{N}_{mn}(\mathbf{r},k)$ obey the homogeneous vectorial wave equation, i.e.,

$$\boldsymbol{\nabla}\times\boldsymbol{\nabla}\times\begin{Bmatrix}\mathbf{M}_{mn}(\mathbf{r},k)\\ \mathbf{N}_{mn}(\mathbf{r},k)\end{Bmatrix}-k^2\begin{Bmatrix}\mathbf{M}_{mn}(\mathbf{r},k)\\ \mathbf{N}_{mn}(\mathbf{r},k)\end{Bmatrix}=0, \tag{37}$$

whereas the same is not true for functions $\mathbf{L}_{mn}(\mathbf{r},k)$. From the definitions, one can readily verify that

$$\boldsymbol{\nabla}\cdot\mathbf{L}_{mn}(\mathbf{r},k)\neq 0, \tag{38}$$

$$\boldsymbol{\nabla}\cdot\begin{Bmatrix}\mathbf{M}_{mn}(\mathbf{r},k)\\ \mathbf{N}_{mn}(\mathbf{r},k)\end{Bmatrix}=0. \tag{39}$$

Owing to these relations, functions $\mathbf{M}_{mn}(\mathbf{r},k)$ and $\mathbf{N}_{mn}(\mathbf{r},k)$ are called transversal (or solenoidal) vector wave functions, whereas $\mathbf{L}_{mn}(\mathbf{r},k)$ is a longitudinal (or irrotational) wave function. Furthermore, since the functions $\phi_{mn}(\mathbf{r},k)$ satisfy the scalar Helmholtz equation, Eq. (12), the vectors in Eqs. (34)–(36) are solutions of the vectorial Helmholtz equation, i.e.,

$$\nabla^2\begin{Bmatrix}\mathbf{L}_{mn}(\mathbf{r},k)\\ \mathbf{M}_{mn}(\mathbf{r},k)\\ \mathbf{N}_{mn}(\mathbf{r},k)\end{Bmatrix}+k^2\begin{Bmatrix}\mathbf{L}_{mn}(\mathbf{r},k)\\ \mathbf{M}_{mn}(\mathbf{r},k)\\ \mathbf{N}_{mn}(\mathbf{r},k)\end{Bmatrix}=0. \tag{40}$$

We also mention the following symmetry relations:

$$\mathbf{M}_{mn}(\mathbf{r},k)=\frac{1}{k}\boldsymbol{\nabla}\times\mathbf{N}_{mn}(\mathbf{r},k), \tag{41}$$

$$\mathbf{N}_{mn}(\mathbf{r},k)=\frac{1}{k}\boldsymbol{\nabla}\times\mathbf{M}_{mn}(\mathbf{r},k). \tag{42}$$

For this work, we need to know the orthogonality relations of the vector wave functions. They are obtained by straightforward, although quite lengthy, calculations outlined in Appendix B. We have included the derivation of the orthogonality relations for completeness, since in our analysis we use a somewhat different form for the functions $\phi_{mn}(\mathbf{r},k)$ than seems to be customary in the literature [20,21]. Often the angular part of $\phi_{mn}(\mathbf{r},k)$ is written in terms of the associated Legendre functions and trigonometric functions, instead of the spherical harmonics that we employ [see Eq. (11)]. Use of trigonometric functions results in two sets of vector wave functions, one of which is even and the other odd in the angular variable φ.

In the sense of Eq. (25), the orthogonality relations in a *finite* spherical volume are of the form (see Appendix B)

$$\{\mathbf{L}_{mn}(\mathbf{r},k),\mathbf{M}_{m'n'}(\mathbf{r},k)\}_D=0, \tag{43}$$

$$\{\mathbf{L}_{mn}(\mathbf{r},k),\mathbf{N}_{m'n'}(\mathbf{r},k)\}_D=n(n+1)\frac{d}{k^2}j_n^2(kd)\,\delta_{mm'}\delta_{nn'}, \tag{44}$$

$$\{\mathbf{M}_{mn}(\mathbf{r},k),\mathbf{N}_{m'n'}(\mathbf{r},k)\}_D=0, \tag{45}$$

$$\{\mathbf{L}_{mn}(\mathbf{r},k),\mathbf{L}_{m'n'}(\mathbf{r},k)\}_D=\left[D_n(k)-\frac{d}{k^2}j_n^2(kd)\right]\delta_{mm'}\delta_{nn'}, \tag{46}$$

$$\{\mathbf{M}_{mn}(\mathbf{r},k),\mathbf{M}_{m'n'}(\mathbf{r},k)\}_D=n(n+1)C_n(k)\,\delta_{mm'}\delta_{nn'}, \tag{47}$$

$$\{\mathbf{N}_{mn}(\mathbf{r},k),\mathbf{N}_{m'n'}(\mathbf{r},k)\}_D=n(n+1)D_n(k)\,\delta_{mm'}\delta_{nn'}, \tag{48}$$

where $C_n(k)$ are the coefficients given in Eq. (14), and

$$D_n(k)=\frac{n+1}{2n+1}C_{n-1}(k)+\frac{n}{2n+1}C_{n+1}(k). \tag{49}$$

We emphasize that the orthogonality properties in Eqs. (43)–(48) again are due to the orthogonality with respect to the angular coordinates only.

In an *infinite* space, the vector wave functions are not only orthogonal in indices m and n, but also with respect to wave number k, which constitutes a continuous set of variables. The orthogonality relations are explicitly written in the form (see Appendix B)

$$\{\mathbf{L}_{mn}(\mathbf{r},k),\mathbf{M}_{m'n'}(\mathbf{r},k')\}_\infty = 0, \tag{50}$$

$$\{\mathbf{L}_{mn}(\mathbf{r},k),\mathbf{N}_{m'n'}(\mathbf{r},k')\}_\infty = 0, \tag{51}$$

$$\{\mathbf{M}_{mn}(\mathbf{r},k),\mathbf{N}_{m'n'}(\mathbf{r},k')\}_\infty = 0, \tag{52}$$

$$\{\mathbf{L}_{mn}(\mathbf{r},k),\mathbf{L}_{m'n'}(\mathbf{r},k')\}_\infty = \frac{\pi}{2}\frac{\delta(k-k')}{k^2}\delta_{mm'}\delta_{nn'}, \tag{53}$$

$$\{\mathbf{M}_{mn}(\mathbf{r},k),\mathbf{M}_{m'n'}(\mathbf{r},k')\}_\infty = n(n+1)\frac{\pi}{2}\frac{\delta(k-k')}{k^2}\delta_{mm'}\delta_{nn'}, \tag{54}$$

$$\{\mathbf{N}_{mn}(\mathbf{r},k),\mathbf{N}_{m'n'}(\mathbf{r},k')\}_\infty = n(n+1)\frac{\pi}{2}\frac{\delta(k-k')}{k^2}\delta_{mm'}\delta_{nn'}, \tag{55}$$

where we have used subscript ∞ to emphasize that they are for an infinite space.

C. Expansion of the infinite-space Green tensor in terms of spherical vector wave functions

In this subsection, the infinite-space Green tensor given in Eq. (32) is expanded in terms of the spherical vector wave functions by means of the Ohm-Rayleigh method [20]. Analogous expansions, in terms of appropriate vector wave functions, are explicitly known for the Green tensors in various geometries, including infinite space. However, we have included the derivation here since the longitudinal vector wave functions $\mathbf{L}_{mn}(\mathbf{r},k)$ are often neglected [20], and because we use spherical harmonics in the $\phi_{mn}(\mathbf{r},k)$ functions leading to orthogonality relations for the vector wave functions that are slightly different from those presented in some publications [20–22].

The infinite-space Green tensor obeys the following two wave equations [20]:

$$\boldsymbol{\nabla}_i \times \boldsymbol{\nabla}_i \times \overleftrightarrow{G}(\mathbf{r}_1,\mathbf{r}_2,k) - k^2\overleftrightarrow{G}(\mathbf{r}_1,\mathbf{r}_2,k) = \delta(\mathbf{r}_1-\mathbf{r}_2)\overleftrightarrow{U}, \quad i=(1,2), \tag{56}$$

where $\boldsymbol{\nabla}_i$ operates on the spatial coordinate $\mathbf{r}_i$ and k is assumed to have a vanishingly small imaginary part. The Dirac δ-function term on the right-hand side can be developed using the vector wave functions whose completeness [25] guarantees the existence of the following expansion:

$$\begin{aligned}\delta(\mathbf{r}_1-\mathbf{r}_2)\overleftrightarrow{U} = &\int_0^\infty \mathrm{d}\kappa \sum_{n=1}^{\infty}\sum_{m=-n}^{n}[\mathbf{M}^*_{mn}(\mathbf{r}_1,\kappa)\mathbf{A}_{mn}(\mathbf{r}_2,\kappa) \\ &+ \mathbf{N}^*_{mn}(\mathbf{r}_1,\kappa)\mathbf{B}_{mn}(\mathbf{r}_2,\kappa)] \\ &+ \int_0^\infty \mathrm{d}\kappa \sum_{n=0}^{\infty}\sum_{m=-n}^{n}\mathbf{L}^*_{mn}(\mathbf{r}_1,\kappa)\mathbf{C}_{mn}(\mathbf{r}_2,\kappa),\end{aligned} \tag{57}$$

where the integration variable is denoted by κ in order to distinguish it from the fixed wave number k. The first sum in the term involving the transversal wave functions starts with 1 since $n=0$ corresponds to a zero term. Using the infinite-space orthogonality relations, Eqs. (50)–(55), we find that

$$\mathbf{A}_{mn}(\mathbf{r},\kappa) = \frac{2}{\pi}\frac{\kappa^2}{n(n+1)}\mathbf{M}_{mn}(\mathbf{r},\kappa), \quad n \geqslant 1, \tag{58}$$

$$\mathbf{B}_{mn}(\mathbf{r},\kappa) = \frac{2}{\pi}\frac{\kappa^2}{n(n+1)}\mathbf{N}_{mn}(\mathbf{r},\kappa), \quad n \geqslant 1, \tag{59}$$

$$\mathbf{C}_{mn}(\mathbf{r},\kappa) = \frac{2\kappa^2}{\pi}\mathbf{L}_{mn}(\mathbf{r},\kappa), \quad n \geqslant 0 \tag{60}$$

leading to the following completeness relationship valid for an infinite space:

$$\begin{aligned}&\delta(\mathbf{r}_1-\mathbf{r}_2)\overleftrightarrow{U} \\ &= \frac{2}{\pi}\int_0^\infty \mathrm{d}\kappa\kappa^2\sum_{n=1}^{\infty}\sum_{m=-n}^{n}\frac{1}{n(n+1)}[\mathbf{M}^*_{mn}(\mathbf{r}_1,\kappa)\mathbf{M}_{mn}(\mathbf{r}_2,\kappa) \\ &\quad + \mathbf{N}^*_{mn}(\mathbf{r}_1,\kappa)\mathbf{N}_{mn}(\mathbf{r}_2,\kappa)] \\ &\quad + \frac{2}{\pi}\int_0^\infty \mathrm{d}\kappa\kappa^2\sum_{n=0}^{\infty}\sum_{m=-n}^{n}\mathbf{L}^*_{mn}(\mathbf{r}_1,\kappa)\mathbf{L}_{mn}(\mathbf{r}_2,\kappa).\end{aligned} \tag{61}$$

For the Green tensor, we consider the following trial expansion:

$$\begin{aligned}&\overleftrightarrow{G}(\mathbf{r}_1,\mathbf{r}_2,k) \\ &= \frac{2}{\pi}\int_0^\infty \mathrm{d}\kappa\kappa^2\sum_{n=1}^{\infty}\sum_{m=-n}^{n}\frac{1}{n(n+1)}[\alpha_{mn}(\kappa,k)\mathbf{M}^*_{mn}(\mathbf{r}_1,\kappa) \\ &\quad \times\mathbf{M}_{mn}(\mathbf{r}_2,\kappa) + \beta_{mn}(\kappa,k)\mathbf{N}^*_{mn}(\mathbf{r}_1,\kappa)\mathbf{N}_{mn}(\mathbf{r}_2,\kappa)] \\ &\quad + \frac{2}{\pi}\int_0^\infty \mathrm{d}\kappa\kappa^2\sum_{n=0}^{\infty}\sum_{m=-n}^{n}\gamma_{mn}(\kappa,k)\mathbf{L}^*_{mn}(\mathbf{r}_1,\kappa)\mathbf{L}_{mn}(\mathbf{r}_2,\kappa).\end{aligned} \tag{62}$$

Inserting this expression and Eq. (61) into Eq. (56), then using Eq. (37), and noting that $\boldsymbol{\nabla}\times\mathbf{L}_{mn}(\mathbf{r},\kappa)=0$ [from the definition (34)], one obtains

$$\alpha_{mn}(\kappa,k)=\beta_{mn}(\kappa,k)=\frac{1}{\kappa^2-k^2}, \tag{63}$$

$$\gamma_{mn}(\kappa,k)=-\frac{1}{k^2}, \tag{64}$$

and therefore

$$\overleftrightarrow{G}(\mathbf{r}_1,\mathbf{r}_2,k)=\frac{2}{\pi}\int_0^\infty \frac{\mathrm{d}\kappa\kappa^2}{\kappa^2-k^2}\sum_{n=1}^{\infty}\sum_{m=-n}^{n}\frac{1}{n(n+1)}[\mathbf{M}^*_{mn}(\mathbf{r}_1,\kappa)\mathbf{M}_{mn}(\mathbf{r}_2,\kappa)+\mathbf{N}^*_{mn}(\mathbf{r}_1,\kappa)\mathbf{N}_{mn}(\mathbf{r}_2,\kappa)]$$
$$-\frac{2}{\pi}\int_0^\infty \frac{\mathrm{d}\kappa\kappa^2}{k^2}\sum_{n=0}^{\infty}\sum_{m=-n}^{n}\mathbf{L}^*_{mn}(\mathbf{r}_1,\kappa)\mathbf{L}_{mn}(\mathbf{r}_2,\kappa). \tag{65}$$

The κ integrations can be carried out analytically as demonstrated in Appendix C. Furthermore, at this stage, we perform the summations in the longitudinal part. These operations [see Eqs. (C1), (C2), (A5), and (C5)] result in the expression

$$\overleftrightarrow{G}(\mathbf{r}_1,\mathbf{r}_2,k)=ik\sum_{n=1}^{\infty}\sum_{m=-n}^{n}\frac{1}{n(n+1)}\begin{cases}\mathbf{M}^*_{mn}(\mathbf{r}_1,k)\mathbf{M}^{(1)}_{mn}(\mathbf{r}_2,k)+\mathbf{N}^*_{mn}(\mathbf{r}_1,k)\mathbf{N}^{(1)}_{mn}(\mathbf{r}_2,k), & r_1<r_2\\ \mathbf{M}^{(2)}_{mn}(\mathbf{r}_1,k)\mathbf{M}_{mn}(\mathbf{r}_2,k)+\mathbf{N}^{(2)}_{mn}(\mathbf{r}_1,k)\mathbf{N}_{mn}(\mathbf{r}_2,k), & r_1>r_2\end{cases}$$
$$-\frac{1}{4\pi k^2}\sum_{n=1}^{\infty}\frac{1}{n(n+1)}(\boldsymbol{\nabla}_1\times\boldsymbol{\nabla}_1\times)(\boldsymbol{\nabla}_2\times\boldsymbol{\nabla}_2\times)\left[\frac{r_<^n}{r_>^{n+1}}P_n(\cos\gamma)\mathbf{r}_1\mathbf{r}_2\right]-\frac{1}{4\pi k^2}\boldsymbol{\nabla}_1\boldsymbol{\nabla}_2\frac{1}{|\mathbf{r}_1-\mathbf{r}_2|}, \tag{66}$$

where $r_<=\min\{|\mathbf{r}_1|,|\mathbf{r}_2|\}$, $r_>=\max\{|\mathbf{r}_1|,|\mathbf{r}_2|\}$, γ is the angle between $\mathbf{r}_1$ and $\mathbf{r}_2$, and

$$\mathbf{M}^{(1)}_{mn}(\mathbf{r},k)=\boldsymbol{\nabla}\times[h^{(1)}_n(kr)Y^m_n(\theta,\varphi)\mathbf{r}], \tag{67}$$

$$\mathbf{M}^{(2)}_{mn}(\mathbf{r},k)=\boldsymbol{\nabla}\times[h^{(1)}_n(kr)Y^{m*}_n(\theta,\varphi)\mathbf{r}], \tag{68}$$

$$\mathbf{N}^{(1)}_{mn}(\mathbf{r},k)=\frac{1}{k}\boldsymbol{\nabla}\times\boldsymbol{\nabla}\times[h^{(1)}_n(kr)Y^m_n(\theta,\varphi)\mathbf{r}], \tag{69}$$

$$\mathbf{N}^{(2)}_{mn}(\mathbf{r},k)=\frac{1}{k}\boldsymbol{\nabla}\times\boldsymbol{\nabla}\times[h^{(1)}_n(kr)Y^{m*}_n(\theta,\varphi)\mathbf{r}]. \tag{70}$$

Note that the vector functions with superscript (1) differ from the wave functions defined in Eqs. (35) and (36) in that they involve spherical Hankel functions instead of spherical Bessel functions. The functions with superscript (2), in addition to containing spherical Hankel functions, involve complex-conjugate spherical harmonics.

D. Coherent-mode representation of the cross-spectral density tensor in Eq. (31)

We are now in a position of constructing, in a finite spherical volume D, the coherent-mode representation of the cross-spectral density tensor that is proportional to the infinite-space Green tensor. We note that the last two terms in Eq. (66) are real, except for the prefactor $1/k^2$, which nevertheless can be treated as a real number when the losses are vanishingly small. Inserting Eq. (66) into Eq. (31) and taking the imaginary part of the remaining terms as outlined in Appendix D, we arrive at the expression

$$\overleftrightarrow{W}(\mathbf{r}_1,\mathbf{r}_2,k)=(4\pi)^2a(k)\sum_{n=1}^{\infty}\sum_{m=-n}^{n}\frac{1}{n(n+1)}$$
$$\times[\mathbf{M}^*_{mn}(\mathbf{r}_1,k)\mathbf{M}_{mn}(\mathbf{r}_2,k)+\mathbf{N}^*_{mn}(\mathbf{r}_1,k)$$
$$\times\mathbf{N}_{mn}(\mathbf{r}_2,k)]. \tag{71}$$

This formula is readily rewritten as

$$\overleftrightarrow{W}(\mathbf{r}_1,\mathbf{r}_2,k)=\sum_{n=1}^{\infty}\sum_{m=-n}^{n}\lambda^{(1)}_n(k)\boldsymbol{\psi}^{(1)*}_{mn}(\mathbf{r}_1,k)\boldsymbol{\psi}^{(1)}_{mn}(\mathbf{r}_2,k)$$
$$+\sum_{n=1}^{\infty}\sum_{m=-n}^{n}\lambda^{(2)}_n(k)\boldsymbol{\psi}^{(2)*}_{mn}(\mathbf{r}_1,k)\boldsymbol{\psi}^{(2)}_{mn}(\mathbf{r}_2,k), \tag{72}$$

where

$$\lambda^{(1)}_n(k)=(4\pi)^2a(k)C_n(k), \tag{73}$$

$$\boldsymbol{\psi}^{(1)}_{mn}(\mathbf{r},k)=\frac{1}{[n(n+1)C_n(k)]^{1/2}}\mathbf{M}_{mn}(\mathbf{r},k), \tag{74}$$

and

$$\lambda^{(2)}_n(k)=(4\pi)^2a(k)D_n(k), \tag{75}$$

$$\boldsymbol{\psi}^{(2)}_{mn}(\mathbf{r},k)=\frac{1}{[n(n+1)D_n(k)]^{1/2}}\mathbf{N}_{mn}(\mathbf{r},k). \tag{76}$$

In these expressions, the parameters $C_n(k)$ and $D_n(k)$ are those defined in Eqs. (14) and (49), respectively. Note that the quantities $\lambda^{(1)}_n(k)$ are the eigenvalues encountered already

in the scalar case, cf. Eq. (18). It follows directly from Eqs. (47) and (48) that, in a finite spherical volume D, $\{\boldsymbol{\psi}_{mn}^{(j)}(\mathbf{r},k),\boldsymbol{\psi}_{m'n'}^{(j)}(\mathbf{r},k)\}_D=\delta_{mm'}\delta_{nn'}$, for $j=(1,2)$. Furthermore, Eq. (45) implies that $\{\boldsymbol{\psi}_{mn}^{(1)}(\mathbf{r},k),\boldsymbol{\psi}_{m'n'}^{(2)}(\mathbf{r},k)\}_D=0$ for all values of the indices. It is now an easy task to verify that $\lambda_n^{(j)}(k)$ and $\boldsymbol{\psi}_{mn}^{(j)}(\mathbf{r},k)$, with $j=(1,2)$, are the [$(2n+1)$-fold degenerate] eigenvalues and orthonormal eigenfunctions of the vectorial Fredholm integral equation given in Eq. (26), with the cross-spectral density tensor of Eq. (71) as the kernel. Therefore, Eq. (72) is, within a finite spherical volume, the coherent-mode representation of the cross-spectral density tensor in Eq. (31).

Consider next the total energy of the field in the spherical volume D. The energy density at a point $\mathbf{r}$ is given by

$$S(\mathbf{r},k)=\mathrm{tr}[\overleftrightarrow{W}(\mathbf{r},\mathbf{r},k)]$$
$$=\sum_{n=1}^{\infty}\sum_{m=-n}^{n}[\lambda_n^{(1)}(k)\boldsymbol{\psi}_{mn}^{(1)*}(\mathbf{r},k)\cdot\boldsymbol{\psi}_{mn}^{(1)}(\mathbf{r},k)$$
$$+\lambda_n^{(2)}(k)\boldsymbol{\psi}_{mn}^{(2)*}(\mathbf{r},k)\cdot\boldsymbol{\psi}_{mn}^{(2)}(\mathbf{r},k)], \quad (77)$$

which, when integrated over the volume D, yields the total energy in D as

$$\int_D S(\mathbf{r},k)\mathrm{d}^3r=\sum_{n=1}^{\infty}(2n+1)[\lambda_n^{(1)}(k)+\lambda_n^{(2)}(k)]. \quad (78)$$

Inserting Eqs. (73) and (75), the first form of Eq. (14), and Eq. (49) into the above formula, rearranging the resulting expression, and then using Eq. (A9), we end up with

$$\int_D S(\mathbf{r},k)\mathrm{d}^3r=8\pi a(k)V_D. \quad (79)$$

Exactly the same result is obtained by first taking the limit $\mathbf{r}_1\to\mathbf{r}_2$ in Eq. (31), giving

$$\overleftrightarrow{W}(\mathbf{r},\mathbf{r},k)=\frac{8\pi a(k)}{3}\overleftrightarrow{U}, \quad (80)$$

and then integrating the trace of $\overleftrightarrow{W}(\mathbf{r},\mathbf{r},k)$ over the volume D.

Figure 1 illustrates the distribution of the eigenvalues given in Eqs. (73) and (75), by showing the behavior of the ratios $\lambda_n^{(1)}(k)/\lambda_1^{(1)}(k)$ (dots) and $\lambda_n^{(2)}(k)/\lambda_1^{(1)}(k)$ (stars) as a function of the mode number n. The lower curve corresponds to a spherical volume of radius $d/\lambda=1000$, whereas the upper curve is for $d/\lambda=1500$. The eigenvalues are plotted only for certain modes; the dots and stars are for $n=\{200,600,1000,\ldots\}$ and $n=\{1,400,800,\ldots\}$, respectively. As discussed earlier in connection with scalar fields, Fig. 1 evidences the fact that the bigger the volume, the more modes, in the electromagnetic case both $\boldsymbol{\psi}_{mn}^{(1)}(\mathbf{r},k)$ and $\boldsymbol{\psi}_{mn}^{(2)}(\mathbf{r},k)$ type, are required to represent the cross-spectral density tensor with a sufficient accuracy. We also observe that, to a good approximation, the number of significant modes, $n_{\max}$, is the same for both types of modes. Furthermore, the ratios $\lambda_n^{(1)}(k)/\lambda_1^{(1)}(k)$ and $\lambda_n^{(2)}(k)/\lambda_1^{(1)}(k)$ are also approximately equal and lie on the same curve for a fixed d,

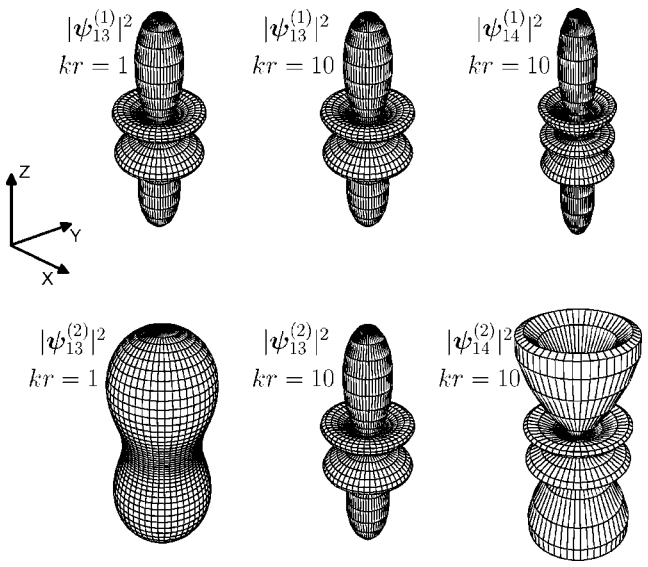

FIG. 3. Illustration of functions $|\boldsymbol{\psi}_{mn}^{(1)}(\mathbf{r},k)|^2$ (upper row) and $|\boldsymbol{\psi}_{mn}^{(2)}(\mathbf{r},k)|^2$ (lower row) for indices $mn=\{13,14\}$, when $kr=1$ and $kr=10$. The radius of the sphere is chosen as $d/\lambda=1000$. The value of the function is indicated by the distance from the origin, which is located in the middle of each graph. The orientation of the coordinate axes is shown in the inset.

although they are strictly different, as can be seen from Eqs. (49), (14), and (A12).

The shapes of the eigenfunctions $\boldsymbol{\psi}_{mn}^{(1)}(\mathbf{r},k)$ and $\boldsymbol{\psi}_{mn}^{(2)}(\mathbf{r},k)$ are demonstrated in Fig. 3 by showing in polar diagrams the behavior of their squared moduli for indices $mn=\{13,14\}$, when $kr=1$ and $kr=10$. The upper and lower rows correspond to functions $\boldsymbol{\psi}_{mn}^{(1)}(\mathbf{r},k)$ and $\boldsymbol{\psi}_{mn}^{(2)}(\mathbf{r},k)$, respectively, and the graphs are for a spherical volume of radius $d/\lambda=1000$. In the direction specified by the angles (θ,φ), the modulus squared of the function is indicated by the distance from the origin, which is located in the center of each graph. We see from Fig. 3 that, when $kr=1$, the absolute values of functions $\boldsymbol{\psi}_{13}^{(1)}(\mathbf{r},k)$ and $\boldsymbol{\psi}_{13}^{(2)}(\mathbf{r},k)$ are markedly different, but for $kr=10$ they are quite similar. In fact, for any mn the squared moduli $|\boldsymbol{\psi}_{mn}^{(1)}(\mathbf{r},k)|^2$ and $|\boldsymbol{\psi}_{mn}^{(2)}(\mathbf{r},k)|^2$ have asymptotically as $kr\to\infty$ the same angular dependence.

E. Degree of coherence of the field represented by the cross-spectral density tensor in Eq. (31)

It is of interest to calculate the electromagnetic degree of coherence as given by Eq. (29) for the field characterized by the electric cross-spectral density tensor in Eq. (31). A direct substitution leads to

$$\mu(\mathbf{r}_1,\mathbf{r}_2,k)=\frac{1}{\sqrt{3}}\left[j_0^2(kR)+\frac{1}{2}j_2^2(kR)\right]^{1/2}, \quad (81)$$

where $R=|\mathbf{r}_1-\mathbf{r}_2|$. We point out that earlier a definition for the *electromagnetic* degree of coherence based on the visibility of intensity fringes in Young's double-slit interference experiment has appeared in the literature [26], evaluated also for blackbody fields [11,15]. This definition results in a sinc function for the degree of coherence, i.e.,

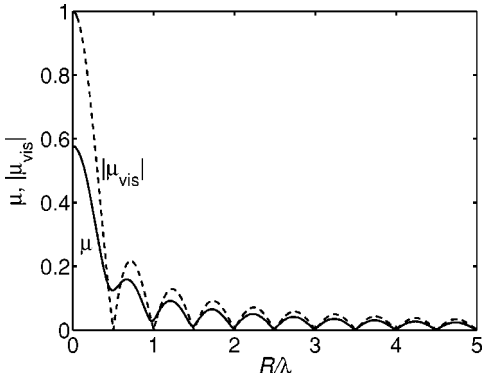

FIG. 4. Behavior of the quantities $\mu(\mathbf{r}_1,\mathbf{r}_2,k)$ [Eq. (81), solid line] and $|\mu_{\mathrm{vis}}(\mathbf{r}_1,\mathbf{r}_2,k)|$ [Eq. (82), dashed line] as a function of R/λ.

$$\mu_{\mathrm{vis}}(\mathbf{r}_1,\mathbf{r}_2,k) = j_0(kR) = \frac{\sin kR}{kR}. \tag{82}$$

The first zero of this function is located at $R=\lambda/2$, demonstrating a generally accepted result that the coherence length of blackbody radiation is on the order of the wavelength for each spectral component. However, the degree of coherence in Eq. (81) qualitatively implies this result as well, as is evidenced by Fig. 4, in which the quantities $\mu(\mathbf{r}_1,\mathbf{r}_2,k)$ and $|\mu_{vis}(\mathbf{r}_1,\mathbf{r}_2,k)|$ are plotted as a function of R/λ. From Fig. 4, or from Eq. (81), we also see that when $\mathbf{r}_1 \to \mathbf{r}_2$, then $\mu(\mathbf{r}_1,\mathbf{r}_2,k) \to 1/\sqrt{3}$. This is due to the fact that blackbody radiation is a fully unpolarized field for which no definite phase relations exist between the three electric-field components at a single point (or between two points). Therefore, for this field, the degree of coherence assumes a value less than unity when $\mathbf{r}_1 \to \mathbf{r}_2$ [19,31].

VI. SUMMARY AND CONCLUSIONS

We constructed, in a finite spherical volume, the coherent-mode representation of specific statistically homogeneous and isotropic scalar fields whose cross-spectral density function is proportional to the imaginary part of the infinite-space Green function. To our knowledge, this is the first three-dimensional scalar coherent-mode representation ever derived. Furthermore, we applied the recently formulated rigorous theory of electromagnetic coherent modes, and developed, in full analogy to the scalar case, the coherent-mode representation for the field whose cross-spectral density tensor is proportional to the infinite-space Green tensor. The results cover the fundamental case of blackbody radiation, but are valid more generally. We also studied the energy distribution among the modes and illustrated, using polar graphs, the geometrical character of some of the lower-order modes.

We point out that two different definitions of the electromagnetic degree of coherence have appeared in the literature, one based on the average correlation between the electric-field components [5,18,19,30] and the other on the visibility of intensity fringes in Young's interference experiment [27–29] (see also Refs. [31,32]). We compared these two degrees of coherence by computing them for the type of homogeneous and isotropic random fields considered in this work, e.g., blackbody radiation. We found that both quantities lead to the conclusion that, for every spectral component, the correlation length in blackbody radiation is on the order of the wavelength. However, only the correlation-based definition of the electromagnetic degree of coherence implies that the elementary modes, i.e., fields for which the cross-spectral density tensor is of a spatially factored form, are fully coherent (and fully polarized). It is our hope that the work presented in this paper inspires further research on the electromagnetic theory of optical coherence, which so far has attracted considerably less attention than the customary scalar coherence theory, but which is of increasing importance in near-field optics, fiber optics, and in the studies dealing with light-matter interactions, for instance.

ACKNOWLEDGMENTS

Financial support from various sources is gratefully acknowledged: T.S. and J.T. thank the Academy of Finland, J.L. the Finnish Cultural Foundation, K.B. Helsinki University of Technology, and A.T.F. the Swedish Research Council. J.T. is also supported by the Alexander von Humboldt Foundation.

APPENDIX A: USEFUL FORMULAS

Orthogonality relation for exponential functions (Eq. 12.141 in Ref. [33]),

$$\int_0^{2\pi} \exp[i(m-m')\varphi]\mathrm{d}\varphi = 2\pi\delta_{mm'}. \tag{A1}$$

Differential equation obeyed by associated Legendre functions (Eq. 12.71 in Ref. [33]),

$$\frac{1}{\sin\theta}\frac{d}{d\theta}\left[\sin\theta\frac{dP_n^m(\cos\theta)}{d\theta}\right] + \left[n(n+1) - \frac{m^2}{\sin^2\theta}\right]P_n^m(\cos\theta) = 0. \tag{A2}$$

Integral involving associated Legendre functions [exercise 12.5.8(a) in Ref. [33]],

$$\int_0^{\pi}\left[\frac{\partial P_n^m(\cos\theta)}{\partial\theta}\frac{\partial P_{n'}^m(\cos\theta)}{\partial\theta} + \frac{m^2}{\sin^2\theta}P_n^m(\cos\theta)P_{n'}^m(\cos\theta)\right]\sin\theta\mathrm{d}\theta = \frac{2n(n+1)}{2n+1}\frac{(n+m)!}{(n-m)!}\delta_{nn'}. \tag{A3}$$

Explicit formula for spherical harmonics $Y_n^m(\theta,\varphi)$ (Eq. 12.146 in Ref. [33]),

$$Y_n^m(\theta,\varphi) = (-1)^m\sqrt{\frac{2n+1}{4\pi}\frac{(n-m)!}{(n+m)!}}P_n^m(\cos\theta)\exp(im\varphi). \tag{A4}$$

Addition theorem for spherical harmonics (Eq. 12.197 in Ref. [33]),

$$P_n(\cos\gamma) = \frac{4\pi}{2n+1}\sum_{m=-n}^{n} Y_n^{m*}(\theta_1,\varphi_1)Y_n^m(\theta_2,\varphi_2), \quad \text{(A5)}$$

where (θ_i,φ_i), with $i=(1,2)$, are the angular coordinates of the position vectors $\mathbf{r}_i$, and γ is the angle between $\mathbf{r}_1$ and $\mathbf{r}_2$.

Normalization and orthogonality relation for spherical harmonics (Eq. 12.147 in Ref. [33]),

$$\int_0^{2\pi}\int_0^{\pi} Y_n^{m*}(\theta,\varphi)Y_{n'}^{m'}(\theta,\varphi)\sin\theta\,\mathrm{d}\theta\mathrm{d}\varphi = \delta_{mm'}\delta_{nn'}. \quad \text{(A6)}$$

Expansion of $1/|\mathbf{r}_1-\mathbf{r}_2|$ in spherical polar coordinates (Eq. 3.70 in Ref. [16]),

$$\frac{1}{|\mathbf{r}_1-\mathbf{r}_2|} = 4\pi\sum_{n=0}^{\infty}\sum_{m=-n}^{n}\frac{1}{2n+1}\frac{r_<^n}{r_>^{n+1}}Y_n^{m*}(\theta_1,\varphi_1)Y_n^m(\theta_2,\varphi_2), \quad \text{(A7)}$$

where $r_<=\min\{|\mathbf{r}_1|,|\mathbf{r}_2|\}$ and $r_>=\max\{|\mathbf{r}_1|,|\mathbf{r}_2|\}$.

Addition theorem for spherical Bessel functions $j_n(r)$ (Eq. 10.1.45 in Ref. [34]),

$$\frac{\sin(k|\mathbf{r}_1-\mathbf{r}_2|)}{k|\mathbf{r}_1-\mathbf{r}_2|} = \sum_{n=0}^{\infty}(2n+1)j_n(kr_1)j_n(kr_2)P_n(\cos\gamma), \quad \text{(A8)}$$

where k is an arbitrary complex number, $r_i=|\mathbf{r}_i|$ for $i=1,2$, and $\gamma=\sphericalangle(\mathbf{r}_1,\mathbf{r}_2)$.

Summation of a series involving $j_n(r)$ (Eq. 10.1.50 in Ref. [34]),

$$\sum_{n=0}^{\infty}(2n+1)j_n^2(kr) = 1, \quad \text{(A9)}$$

for all k.

Two integrals involving spherical Bessel functions (Eq. 3–26 in Ref. [20], Eq. 68 in Appendix D of Ref. [35]),

$$\int_0^{\infty} r^2 j_n(kr)j_n(k'r)\mathrm{d}r = \frac{\pi}{2}\frac{\delta(k-k')}{k^2}, \quad \text{(A10)}$$

$$\int_0^{r} r'^2 j_n^2(kr')\mathrm{d}r' = \frac{r^3}{2}[j_n^2(kr) - j_{n-1}(kr)j_{n+1}(kr)]. \quad \text{(A11)}$$

Two recurrence relations for spherical Bessel functions (Eqs. 10.1.19 and 10.1.20 in Ref. [34]),

$$j_{n-1}(r) + j_{n+1}(r) = (2n+1)\frac{j_n(r)}{r}, \quad \text{(A12)}$$

$$nj_{n-1}(r) - (n+1)j_{n+1}(r) = (2n+1)\frac{\partial j_n(r)}{\partial r}. \quad \text{(A13)}$$

Asymptotic formulas for spherical Bessel functions (Eqs. 11.156 and 11.158 in Ref. [33]),

$$j_n(r) \sim \frac{2^n n!}{(2n+1)!}r^n \quad \text{when } r\to 0, \quad \text{(A14)}$$

$$j_n(r) \sim \frac{1}{r}\sin\left(r-\frac{n\pi}{2}\right) \quad \text{when } r\to\infty. \quad \text{(A15)}$$

Small-argument expansion for spherical Neumann function (Eqs. 11.157 in Ref. [33]),

$$n_n(r) \sim -\frac{(2n)!}{2^n n!}r^{-n-1} \quad \text{when } r\to 0. \quad \text{(A16)}$$

Integral involving spherical Bessel functions (Eqs. 4–14 and 4–16 Ref. [20]),

$$\int_0^{\infty}\frac{F(\kappa)j_n(\kappa r_1)j_n(\kappa r_2)}{\kappa^2-k^2}\mathrm{d}\kappa = \frac{i\pi F(k)}{2k}j_n(kr_<)h_n^{(1)}(kr_>), \quad \text{(A17)}$$

where $r_<=\min\{|\mathbf{r}_1|,|\mathbf{r}_2|\}$ and $r_>=\max\{|\mathbf{r}_1|,|\mathbf{r}_2|\}$. Furthermore, $h_n^{(1)}(r)=j_n(r)+in_n(r)$, where $n_n(r)$ is the spherical Neumann function, is the spherical Hankel function of the first kind. The above equation holds assuming that $F(\kappa)$ is an even function of κ, $F(\kappa)/\kappa$ is an analytic function in the κ plane, and that k has a positive imaginary part.

Special case of the above integral for spherical Bessel functions, with $F(\kappa)=1$,

$$\int_0^{\infty}\frac{j_n(\kappa r_1)j_n(\kappa r_2)}{\kappa^2-k^2}\mathrm{d}\kappa = \frac{i\pi}{2k}j_n(kr_<)h_n^{(1)}(kr_>) - \frac{\pi}{2(2n+1)k^2}\frac{r_<^n}{r_>^{n+1}}. \quad \text{(A18)}$$

This result is obtained analogously to Eq. (A17), but noting in the derivation that when $j_n(\kappa r_2)$ is expressed in terms of the first- and second-order spherical Hankel functions, a first-order pole at $\kappa=0$ is present, and needs to be taken into account.

Operators $\boldsymbol{\nabla}$ and $\boldsymbol{\nabla}\times\mathbf{A}$ in spherical polar coordinates,

$$\boldsymbol{\nabla} = \hat{r}\frac{\partial}{\partial r} + \frac{\hat{\theta}}{r}\frac{\partial}{\partial\theta} + \frac{\hat{\varphi}}{r\sin\theta}\frac{\partial}{\partial\varphi}, \quad \text{(A19)}$$

$$\boldsymbol{\nabla}\times\mathbf{A} = \frac{1}{r\sin\theta}\left[\frac{\partial(\sin\theta A_\varphi)}{\partial\theta} - \frac{\partial A_\theta}{\partial\varphi}\right]\hat{r} + \left[\frac{1}{r\sin\theta}\frac{\partial A_r}{\partial\varphi} - \frac{1}{r}\frac{\partial(rA_\varphi)}{\partial r}\right]\hat{\theta} + \frac{1}{r}\left[\frac{\partial(rA_\theta)}{\partial r} - \frac{\partial A_r}{\partial\theta}\right]\hat{\varphi}, \quad \text{(A20)}$$

where $(\hat{r},\hat{\theta},\hat{\varphi})$ are the unit vectors along the axes of the coordinate system.

APPENDIX B: ORTHOGONALITY OF SPHERICAL VECTOR WAVE FUNCTIONS

The orthogonality relations are computed by substituting into Eq. (25) the explicit forms of the vector wave functions, which with the help of Eqs. (A19) and (A20) are found to be

$$\mathbf{L}_{mn}(\mathbf{r},k)=\frac{1}{k}\frac{\partial j_n(kr)}{\partial r}Y_n^m(\theta,\varphi)\hat{r}+\frac{j_n(kr)}{kr}\left[\frac{\partial Y_n^m(\theta,\varphi)}{\partial\theta}\hat{\theta}+\frac{im}{\sin\theta}Y_n^m(\theta,\varphi)\hat{\varphi}\right], \tag{B1}$$

$$\mathbf{M}_{mn}(\mathbf{r},k)=j_n(kr)\left[\frac{im}{\sin\theta}Y_n^m(\theta,\varphi)\hat{\theta}-\frac{\partial Y_n^m(\theta,\varphi)}{\partial\theta}\hat{\varphi}\right], \tag{B2}$$

$$\mathbf{N}_{mn}(\mathbf{r},k)=\frac{n(n+1)}{kr}j_n(kr)Y_n^m(\theta,\varphi)\hat{r}+\frac{1}{kr}\frac{\partial}{\partial r}[rj_n(kr)]\times\left[\frac{\partial Y_n^m(\theta,\varphi)}{\partial\theta}\hat{\theta}+\frac{im}{\sin\theta}Y_n^m(\theta,\varphi)\hat{\varphi}\right]. \tag{B3}$$

In obtaining the last equation, Eq. (A2) is particularly useful. Note that $\mathbf{M}_{00}(\mathbf{r},k)=\mathbf{N}_{00}(\mathbf{r},k)=0$ [since $P_0^0(\cos\theta)=1$].

The following integral appears often in deriving the orthogonality relations, and is given here for convenience:

$$\int_0^{2\pi}\int_0^{\pi}\left[\frac{m}{\sin\theta}Y_n^{m*}(\theta,\varphi)\frac{\partial Y_{n'}^{m'}(\theta,\varphi)}{\partial\theta}+\frac{m'}{\sin\theta}\frac{Y_n^{m*}(\theta,\varphi)}{\partial\theta}Y_{n'}^{m'}(\theta,\varphi)\right]\sin\theta\,\mathrm{d}\theta\mathrm{d}\varphi=0, \tag{B4}$$

which holds for all m,m',n,n'. This formula is obtained by substituting from Eq. (A4) for spherical harmonics, carrying out the resulting φ integration using Eq. (A1), and then noting that for associated Legendre functions $P_n^m(\pm1)=0$ for $m\neq0$ (Eq. 12.91 in Ref. [33]). Equation (B4) can be verified also for index $m=0$. Another integral involving angular coordinates that is frequently encountered is of the form

$$\int_0^{2\pi}\int_0^{\pi}\left[\frac{\partial Y_n^{m*}(\theta,\varphi)}{\partial\theta}\frac{\partial Y_{n'}^{m'}(\theta,\varphi)}{\partial\theta}+\frac{mm'}{\sin^2\theta}Y_n^{m*}(\theta,\varphi)Y_{n'}^{m'}(\theta,\varphi)\right]\sin\theta\,\mathrm{d}\theta\mathrm{d}\varphi=n(n+1)\delta_{nn'}\delta_{mm'}, \tag{B5}$$

which is obtained straightforwardly by using Eqs. (A4), (A1), and (A3).

We need also the following two relations involving spherical Bessel functions. First,

$$n(n+1)j_n(kr)j_n(k'r)+\frac{\partial}{\partial r}[rj_n(kr)]\frac{\partial}{\partial r}[rj_n(k'r)]=\frac{kk'r^2}{2n+1}[(n+1)j_{n-1}(kr)j_{n-1}(k'r)+nj_{n+1}(kr)j_{n+1}(k'r)], \tag{B6}$$

which is directly verified by using Eqs. (A12) and (A13) on the left-hand side. Second,

$$r^2\frac{\partial j_n(kr)}{\partial r}\frac{\partial j_n(k'r)}{\partial r}=\frac{\partial}{\partial r}[rj_n(kr)]\frac{\partial}{\partial r}[rj_n(k'r)]-\frac{\partial}{\partial r}[rj_n(kr)j_n(k'r)], \tag{B7}$$

which, in turn, is verified on performing the derivatives on the right-hand side. Note that in the above equations, the argument of Bessel functions is kr rather than r, which is present in the recurrence relations.

Orthogonality relations in Eqs. (43), (45), (50), and (52)

The orthogonality relations in Eqs. (43), (45), (50), and (52) are readily obtained by using Eqs. (B1)–(B3) in Eq. (25), and noting that in all cases we end up with the angular integration of Eq. (B4).

Orthogonality relations in Eqs. (44) and (51)

Use of Eqs. (B1) and (B3) in Eq. (25) straightforwardly leads to

$$\{\mathbf{L}_{mn}(\mathbf{r},k),\mathbf{N}_{m'n'}(\mathbf{r},k')\}_D=\frac{n(n+1)}{kk'}\Big|_0^d rj_n(kr)j_n(k'r)\delta_{mm'}\delta_{nn'}. \tag{B8}$$

The angular integrations encountered in deriving this result are exactly those of Eqs. (A6) and (B5). Employing the asymptotic forms of spherical Bessel functions, Eqs. (A14) and (A15), we obtain the orthogonality relations given in Eqs. (44) and (51).

Orthogonality relations in Eqs. (46) and (53)

Substituting Eq. (B1) into Eq. (25), performing the angular integrations with the help of Eqs. (A6) and (B5), we find that

$$\{\mathbf{L}_{mn}(\mathbf{r},k),\mathbf{L}_{m'n'}(\mathbf{r},k')\}_D=\frac{1}{kk'}\int_0^d\left[r^2\frac{\partial j_n(kr)}{\partial r}\frac{\partial j_n(k'r)}{\partial r}+n(n+1)j_n(kr)j_n(k'r)\right]\times\mathrm{d}r\,\delta_{mm'}\delta_{nn'}. \tag{B9}$$

Next we note that using Eqs. (B6) and (B7), this equation can be arranged as

$$\{\mathbf{L}_{mn}(\mathbf{r},k),\mathbf{L}_{m'n'}(\mathbf{r},k')\}_D=\frac{n+1}{2n+1}\int_0^d r^2j_{n-1}(kr)j_{n-1}(k'r)\mathrm{d}r\,\delta_{mm'}\delta_{nn'}+\frac{n}{2n+1}\int_0^d r^2j_{n+1}(kr)j_{n+1}(k'r)\mathrm{d}r\,\delta_{mm'}\delta_{nn'}-\frac{1}{kk'}\Big|_0^d rj_n(kr)j_n(k'r)\delta_{mm'}\delta_{nn'}. \tag{B10}$$

This form, with the help of Eqs. (14), (49), (A10), (A14), and

(A15), implies the orthogonality relations in Eqs. (46) and (53).

Orthogonality relations in Eqs. (47) and (54)

The orthogonality relations, Eqs. (47) and (54), for the functions $\mathbf{M}_{mn}(\mathbf{r},k)$ defined by Eq. (B2), are obtained from

$$\{\mathbf{M}_{mn}(\mathbf{r},k),\mathbf{M}_{m'n'}(\mathbf{r},k')\}_D = n(n+1)\int_0^d r^2 j_n(kr)j_n(k'r)\mathrm{d}r\,\delta_{mm'}\delta_{nn'}. \quad \text{(B11)}$$

The angular integration encountered in the derivation of this formula is the one given in Eq. (B5). Making use of Eqs. (14) and (A10) at once results in Eqs. (47) and (54).

Orthogonality relations in Eqs. (48) and (55)

Inserting Eq. (B3) into Eq. (25), performing the angular integrations using Eqs. (A6) and (B6), we find that

$$\{\mathbf{N}_{mn}(\mathbf{r},k),\mathbf{N}_{m'n'}(\mathbf{r},k')\}_D = \frac{n(n+1)}{kk'}\int_0^d \left\{ n(n+1)j_n(kr)j_n(k'r) + \frac{\partial}{\partial r}[rj_n(kr)]\frac{\partial}{\partial r}[rj_n(k'r)]\right\}\mathrm{d}r\,\delta_{mm'}\delta_{nn'}. \quad \text{(B12)}$$

Employing Eq. (B2), this formula takes on the form

$$\{\mathbf{N}_{mn}(\mathbf{r},k),\mathbf{N}_{m'n'}(\mathbf{r},k')\}_D = \frac{n(n+1)^2}{2n+1}\int_0^d r^2 j_{n-1}(kr)j_{n-1}(k'r)\mathrm{d}r\,\delta_{mm'}\delta_{nn'} + \frac{n^2(n+1)}{2n+1}\int_0^d r^2 j_{n+1}(kr)j_{n+1}(k'r)\mathrm{d}r\,\delta_{mm'}\delta_{nn'}. \quad \text{(B13)}$$

We see that use of Eqs. (14), (49), and (A10) in the above formula leads to the orthogonality relations given in Eqs. (48) and (55).

APPENDIX C: SIMPLIFICATION OF EQ. (65)

κ integration for the $\mathbf{M}_{mn}(\mathbf{r},\kappa)$-function part

First making use of Eqs. (35) and (11), and then Eq. (A17), one obtains

$$\begin{aligned}
&\frac{2}{\pi}\int_0^\infty \frac{\mathrm{d}\kappa\kappa^2}{\kappa^2-k^2}\sum_{n=1}^\infty\sum_{m=-n}^n \frac{1}{n(n+1)}\mathbf{M}^*_{mn}(\mathbf{r}_1,\kappa)\mathbf{M}_{mn}(\mathbf{r}_2,\kappa)\\
&\quad=\frac{2}{\pi}\sum_{n=1}^\infty\sum_{m=-n}^n \frac{1}{n(n+1)}(\nabla_1\times)(\nabla_2\times)\int_0^\infty \frac{\mathrm{d}\kappa\kappa^2 j_n(\kappa r_1)j_n(\kappa r_2)}{\kappa^2-k^2}[Y_n^{m*}(\theta_1,\varphi_1)\mathbf{r}_1][Y_n^m(\theta_2,\varphi_2)\mathbf{r}_2]\\
&\quad=ik\sum_{n=1}^\infty\sum_{m=-n}^n \frac{1}{n(n+1)}\begin{cases}\nabla_1\times[j_n(kr_1)Y_n^{m*}(\theta_1,\varphi_1)\mathbf{r}_1]\nabla_2\times[h_n^{(1)}(kr_2)Y_n^m(\theta_2,\varphi_2)\mathbf{r}_2], & r_1<r_2\\ \nabla_1\times[h_n^{(1)}(kr_1)Y_n^{m*}(\theta_1,\varphi_1)\mathbf{r}_1]\nabla_2\times[j_n(kr_2)Y_n^m(\theta_2,\varphi_2)\mathbf{r}_2], & r_1>r_2,\end{cases}
\end{aligned} \quad \text{(C1)}$$

where $\nabla_i\times$, with $i=(1,2)$, operates on the vector $\mathbf{r}_i$.

κ integration for the $\mathbf{N}_{mn}(\mathbf{r},\kappa)$-function part

Employing Eqs. (36) and (11), and then Eq. (A18), after straightforward computations one finds that

$$\begin{aligned}
&\frac{2}{\pi}\int_0^\infty \frac{\mathrm{d}\kappa\kappa^2}{\kappa^2-k^2}\sum_{n=1}^\infty\sum_{m=-n}^n \frac{1}{n(n+1)}\mathbf{N}^*_{mn}(\mathbf{r}_1,\kappa)\mathbf{N}_{mn}(\mathbf{r}_2,\kappa)\\
&\quad=\frac{2}{\pi}\sum_{n=1}^\infty\sum_{m=-n}^n \frac{1}{n(n+1)}(\nabla_1\times\nabla_1\times)(\nabla_2\times\nabla_2\times)\int_0^\infty \frac{\mathrm{d}\kappa j_n(\kappa r_1)j_n(\kappa r_2)}{\kappa^2-k^2}[Y_n^{m*}(\theta_1,\varphi_1)\mathbf{r}_1][Y_n^m(\theta_2,\varphi_2)\mathbf{r}_2]\\
&\quad=\frac{i}{k}\sum_{n=1}^\infty\sum_{m=-n}^n \frac{1}{n(n+1)}\begin{cases}\nabla_1\times\nabla_1\times[j_n(kr_1)Y_n^{m*}(\theta_1,\varphi_1)\mathbf{r}_1]\nabla_2\times\nabla_2\times[h_n^{(1)}(kr_2)Y_n^m(\theta_2,\varphi_2)\mathbf{r}_2], & r_1<r_2\\ \nabla_1\times\nabla_1\times[h_n^{(1)}(kr_1)Y_n^{m*}(\theta_1,\varphi_1)\mathbf{r}_1]\nabla_2\times\nabla_2\times[j_n(kr_2)Y_n^m(\theta_2,\varphi_2)\mathbf{r}_2], & r_1>r_2\end{cases}\\
&\qquad-\sum_{n=1}^\infty\sum_{m=-n}^n \frac{1}{n(n+1)}(\nabla_1\times\nabla_1\times)(\nabla_2\times\nabla_2\times)\times\left\{\frac{1}{(2n+1)k^2}\frac{r_<^n}{r_>^{n+1}}[Y_n^{m*}(\theta_1,\varphi_1)\mathbf{r}_1][Y_n^m(\theta_2,\varphi_2)\mathbf{r}_2]\right\},
\end{aligned} \quad \text{(C2)}$$

where $\nabla_i\times$, with $i=(1,2)$, operates on the vector $\mathbf{r}_i$, and $r_<=\min\{|\mathbf{r}_1|,|\mathbf{r}_2|\}$ and $r_>=\max\{|\mathbf{r}_1|,|\mathbf{r}_2|\}$. We point out that in Ref. [20] (p. 173) the pole at $\kappa=0$ is not taken into account and, consequently, the last term of Eq. (C2) is missing in that work

(noted also on p. 190 in Ref. [21]).

κ integration and summations for the $\mathbf{L}_{mn}(\mathbf{r},\kappa)$-function part

Making use of Eq. (34), we obtain

$$\frac{2}{\pi}\int_0^\infty \frac{\mathrm{d}\kappa\kappa^2}{k^2}\sum_{n=0}^{\infty}\sum_{m=-n}^{n}\mathbf{L}^*_{mn}(\mathbf{r}_1,\kappa)\mathbf{L}_{mn}(\mathbf{r}_2,\kappa),$$
$$=\frac{2}{\pi k^2}\nabla_1\nabla_2\sum_{n=0}^{\infty}\sum_{m=-n}^{n}\int_0^\infty \mathrm{d}\kappa j_n(\kappa r_1)j_n(\kappa r_2)$$
$$\times[Y_n^{m*}(\theta_1,\varphi_1)Y_n^m(\theta_2,\varphi_2)]. \tag{C3}$$

The κ integration can be performed as follows:

$$\int_0^\infty \mathrm{d}\kappa j_n(\kappa r_1)j_n(\kappa r_2)$$
$$=\lim_{\delta\to 0}\int_0^\infty \frac{\kappa^2 j_n(\kappa r_1)j_n(\kappa r_2)\mathrm{d}\kappa}{\kappa^2-(i\delta)^2},$$
$$=-\lim_{\delta\to 0}\frac{\pi\delta}{2}j_n(i\delta r_<)h_n^{(1)}(i\delta r_>),$$
$$=\frac{\pi}{2}\frac{r_<^n}{(2n+1)r_>^{n+1}}, \tag{C4}$$

where the second expression follows from Eq. (A17), whereas the third is obtained from Eqs. (A14) and (A16). Employing Eqs. (C4) and (A7) results in the expression

$$\frac{2}{\pi}\int_0^\infty \frac{\mathrm{d}\kappa\kappa^2}{k^2}\sum_{n=0}^{\infty}\sum_{m=-n}^{n}\mathbf{L}^*_{mn}(\mathbf{r}_1,\kappa)\mathbf{L}_{mn}(\mathbf{r}_2,\kappa)$$
$$=\frac{1}{4\pi k^2}\boldsymbol{\nabla}_1\boldsymbol{\nabla}_2\frac{1}{|\mathbf{r}_1-\mathbf{r}_2|} \tag{C5}$$

for the longitudinal part of the infinite-space Green tensor.

APPENDIX D: IMAGINARY PART OF INFINITE-SPACE GREEN TENSOR

Computation of the imaginary part of the tensor in Eq. (66) is demonstrated here only for the sum containing $\mathbf{M}^*_{mn}(\mathbf{r},\kappa)\mathbf{M}^{(1)}_{mn}(\mathbf{r},\kappa)$ terms. A straightforward calculation leads to

$$\mathrm{Im}\left[ik\sum_{n=1}^{\infty}\sum_{m=-n}^{n}\frac{1}{n(n+1)}\mathbf{M}^*_{mn}(\mathbf{r}_1,k)\mathbf{M}^{(1)}_{mn}(\mathbf{r}_2,k)\right]$$
$$=\mathrm{Re}\left\{k\sum_{n=1}^{\infty}\frac{1}{n(n+1)}(\nabla_1\times)(\nabla_2\times)\right.$$
$$\left.\times\sum_{m=-n}^{n}Y_n^{m*}(\theta_1,\varphi_1)Y_n^m(\theta_2,\varphi_2)[j_n(kr_1)\mathbf{r}_1][h_n^{(1)}(kr_2)\mathbf{r}_2]\right\},$$
$$=k\sum_{n=1}^{\infty}\sum_{m=-n}^{n}\frac{1}{n(n+1)}\mathbf{M}^*_{mn}(\mathbf{r}_1,k)\mathbf{M}_{mn}(\mathbf{r}_2,k). \tag{D1}$$

Here the second expression results from Eqs. (35) and (67). The third expression is obtained by noting that according to Eq. (A5), the sum involving spherical harmonics is purely real, and recalling that $\mathrm{Re}[h_n^{(1)}(kr)]\approx j_n(kr)\approx\mathrm{Re}[j_n(kr)]$ when k has a vanishingly small imaginary part.

The sums involving other terms are treated in full analogy. It is readily verified that the computation of the imaginary part of Eq. (66) is formally the same as replacing the functions $\mathbf{M}^{(1)}_{mn}(\mathbf{r},k)$ and $\mathbf{M}^{(2)}_{mn}(\mathbf{r},k)$ with $\mathbf{M}_{mn}(\mathbf{r},k)$, and the functions $\mathbf{N}^{(1)}_{mn}(\mathbf{r},k)$ and $\mathbf{N}^{(2)}_{mn}(\mathbf{r},k)$ with $\mathbf{N}_{mn}(\mathbf{r},k)$.

[1] L. Mandel and E. Wolf, *Optical Coherence and Quantum Optics* (Cambridge University Press, Cambridge, UK, 1995).
[2] E. Wolf, J. Opt. Soc. Am. **72**, 343 (1982).
[3] D. Cabaret, S. Rossano, and C. Brouder, Opt. Commun. **150**, 239 (1998).
[4] S. Withington, G. Yassin, J. A. Murphy, IEEE Trans. Antennas Propag. **49**, 1226 (2001).
[5] J. Tervo, T. Setälä, and A. T. Friberg, J. Opt. Soc. Am. A **21**, 2205 (2004).
[6] F. Gori, M. Santarsiero, R. Simon, G. Piquero, R. Borghi, and G. Guattari, J. Opt. Soc. Am. A **20**, 78 (2003).
[7] H. M. Nussenzveig, J. T. Foley, K. Kim, and E. Wolf, Phys. Rev. Lett. **58**, 218 (1987).
[8] S. A. Ponomarenko and E. Wolf, Phys. Rev. E **65**, 016602 (2001).
[9] J. T. Foley, W. H. Carter, and E. Wolf, J. Opt. Soc. Am. A **3**, 1090 (1986).
[10] T. Setälä, K. Blomstedt, M. Kaivola, and A. T. Friberg, Phys. Rev. E **67**, 026613 (2003).
[11] W. H. Carter and E. Wolf, J. Opt. Soc. Am. **65**, 1067 (1975).
[12] C. L. Mehta and E. Wolf, Phys. Rev. **161**, 1328 (1967).
[13] G. S. Agarwal, Phys. Rev. A **11**, 230 (1975).
[14] F. Gori, D. Ambrosini, and V. Bagini, Opt. Commun. **107**, 331 (1994).
[15] T. Setälä, M. Kaivola, and A. T. Friberg, Opt. Lett. **28**, 1069 (2003).
[16] J. D. Jackson, *Classical Electrodynamics* 3rd ed. (Wiley, New York, 1999).
[17] T. Setälä, A. Shevchenko, M. Kaivola, and A. T. Friberg, Phys. Rev. E **66**, 016615 (2003).
[18] T. Setälä, J. Tervo, and A. T. Friberg, Opt. Lett. **29**, 328 (2004).

[19] J. Tervo, T. Setälä, and A. T. Friberg, Opt. Express **11**, 1137 (2003).
[20] C.-T. Tai, *Dyadic Green's Functions in Electromagnetic Theory* (Intext, Scranton, PA, 1971).
[21] R. E. Collin, Electromagnetics **6**, 183 (1986).
[22] D. N. J. Wall, J. Phys. A **11**, 749 (1978).
[23] P. Morse and H. Feshbach, *Methods of Theoretical Physics* (McGraw-Hill, New York, 1953).
[24] L.-W. Li, X.-K. Kang, and M.-S. Leong, *Spheroidal Wave Functions in Electromagnetic Theory* (Wiley, New York, 2001).
[25] W. W. Hansen, Phys. Rev. **47**, 139 (1934).
[26] This definition was originally formulated in the space-time domain by Karczewski in 1963 [27]. A space-frequency analogue of this degree of electromagnetic coherence was employed in radiation analysis [28] and later, in 2003, it was formalized by Wolf for electromagnetic beams in a two-pinhole interference geometry [29]. Visibility as a definition of the *electromagnetic* degree of coherence was recently questioned [5,18,19,30], and actively discussed [31,32].
[27] B. Karczewski, Phys. Lett. **5**, 191 (1963); B. Karczewski, Nuovo Cimento **30**, 906 (1963).
[28] W. H. Carter and E. Wolf, Phys. Rev. A **36**, 1258 (1987).
[29] E. Wolf, Phys. Lett. A **312**, 263 (2003).
[30] T. Setälä, J. Tervo, and A. T. Friberg, Opt. Commun. **238**, 229 (2004).
[31] E. Wolf, Opt. Lett. **29**, 1712 (2004); T. Setälä, J. Tervo, and A. T. Friberg, *ibid.* **29**, 1713 (2004).
[32] E. Wolf, Opt. Commun. **242**, 321 (2004); T. Saastamoinen, J. Tervo, and J. Turunen, *ibid.* **242**, 323 (2004).
[33] G. Arfken, *Mathematical Methods for Physicists* 3rd ed. (Academic Press, San Diego, 1985).
[34] *Handbook of Mathematical Functions*, edited by M. Abramowitz and I. A. Stegun (Dover, New York, 1972).
[35] J. VanBladel, *Electromagnetic Fields* (McGraw-Hill, New York, 1964).